ELSEVIER

Journal of Photochemistry and Photobiology A: Chemistry 95 (1996) 115–125

Journal of PHOTOCHEMISTRY AND PHOTOBIOLOGY A:CHEMISTRY

Spectroscopy of *o*-diazahelicenes of C_{2v}/C_2 symmetry

Gerhard Greiner [a,*], Hermann Rau [a], Roland Bonneau [b]

[a] *Institut für Chemie, FG Physikalische Chemie, Universität Hohenheim, 70593 Stuttgart, Germany*

[b] *Laboratoire de Photophysique et Photochimie Moléculaire, CNRS UA 248, Université de Bordeaux I, 33405 Talence, France*

Received 31 August 1994; accepted 6 October 1995

Abstract

The absorption and emission properties of members of the series benzo[c]cinnoline ("diazatrishelicene"), diazapentahelicene and diazadibenzoheptahelicene change in a characteristic way. The solvent properties influence strongly the phosphorescence/fluorescence ratio. For heptahelicene, this ratio shows an intricate dependence on the excitation wavelength, which has not been observed previously. A common feature is the very low emission yield. The energies of the excited (n,π^*) and (π,π^*) states of non-planar pentahelicene and heptahelicene are crucial for these properties; very effective radiationless deactivation of the lowest triplet states, presumably due to a pseudo-Jahn–Teller effect, is observed. Good agreement is found between the empirical and calculated sequences in the energy diagram of the excited states.

Keywords: Fluorescence; Phosphorescence; Quantum yield; Solvent effect

1. Introduction

For several years, we have been interested in the spectroscopic properties of azo compounds. Reviews have been given recently [1]. Azo compounds are characterized by strong coupling of the n electrons carried by neighbouring N atoms; this leads to n_s–n_a splitting of up to 26 000 cm^{-1}, as observed by photoelectron spectroscopy for azomethane [2], and consequently low-lying (n,π^*) states. In aromatic azo compounds, the (π,π^*) states lie between the two (n,π^*) states on the energy scale, thus decreasing the gap between the lowest excited states. We have classified the azobenzenes according to this gap: azobenzene-type ($(n,\pi^*) < (\pi,\pi^*)$); aminoazobenzene-type ($(n,\pi^*) \approx (\pi,\pi^*)$); pseudo-stilbenes ($(n,\pi^*) > (\pi,\pi^*)$) [1].

Azobenzene is characterized by a large $^1(n,\pi^*)$–$^1(\pi,\pi^*)$ gap of 9000–10 000 cm^{-1}. Such a gap is not easily bridged in a rigid molecule. However, azobenzene is very floppy and deactivates by *Z–E* isomerization via rotation in the (π,π^*) and inversion in the (n,π^*) states [3]. Therefore no emission is found, either in the *E* isomer where the $n \rightarrow \pi^*$ transition is forbidden (C_{2h}) or in the *Z* isomer where it would be allowed (C_{2v}). Special structures are needed to induce emission in azobenzene-type azo compounds [4–6]. One such property is structural rigidity, which can be provided by an *o*-diazaaromatic ring system. Of course, in such a ring system, only the *Z* structure can be stabilized and the π electronic system differs from that of the corresponding aromatic azo compound and resembles that of the corresponding aromatic hydrocarbon. Nevertheless, the absorption spectrum of benzo[c]cinnoline (**1**) can easily be related to those of azobenzene and phenanthrene.

The (n,π^*)–(π,π^*) gap of azobenzene can be modified by electron-donating and electron-withdrawing substituents, but also by an extension of the aromatic system. In this study, we used the latter principle, and selected a series of three molecules which are representatives of the three classes of azo compounds defined above (see Scheme 1).

We investigated both theoretically and experimentally the excited states of these systems and the dependence of their

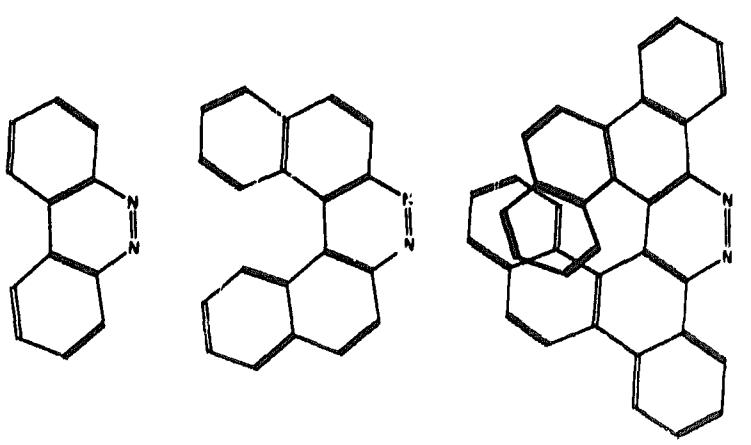

1 2 3

Scheme 1.

* Corresponding author.

1010-6030/96/$15.00 © 1996 Elsevier Science S.A. All rights reserved
SSDI 1010-6030(95)04246-6

spectral properties on the solvent polarity and excitation wavelength. Our interest in the latter issue was initiated by a paper by O'Dwyer et al. [7] reporting that, for the hydrocarbon hexahelicene, the phosphorescence/fluorescence (P/F) ratio should be wavelength dependent. However, in a parallel study, we were unable to confirm this result [8]; nevertheless the P/F properties of **3** were surprising. Moreover, the helicenes are chiral, and circular dichroism (CD) spectra may contain more information for excited state assignment than UV spectra.

2. Experimental section

2.1. Materials

1 was produced from 1,1′-dinitrobiphenyl by electrochemical reduction [9]. For comparison, we also synthesized **1** by photodehydrocyclization of azobenzene in 66% H_2SO_4 [10]. The material was purified by column chromatography on SiO_2 and recrystallized from hexane immediately before use. Thin layer chromatographic purity was a criterion.

2 was prepared by photodehydrocyclization from 2,2′-azonaphthalene in H_2SO_4 (m.p., 273 °C), and was identified by comparison of the absorption spectrum with those given in Refs. [11] and [12] and by comparison of the retention time on a silicate column modified by chiral TAPA with that of **3** [13]. Resolution of the racemic pentahelicene was not possible [13]. The material was purified by thick layer chromatography for the spectroscopic experiments; the purity was checked by thin layer chromatography.

In contrast with the literature, the cyclization of 2,2′-azonaphthalene in $AlCl_3/ZnCl_2$ melt [14] yielded a different product with an absorption spectrum typical of an aromatic hydrocarbon. We assign this compound as pyridazino-[ghi]perylene, the cyclodehydration product of **2**, due to the close relationship of its UV spectrum with that of benzo[ghi]perylene [15].

The preparation of **3** by cyclization of 6,6′-azochrysene in H_2SO_4 and its purification have been reported previously [16].

Molecules whose triplet states should be quenched by **1**, **2** or **3** were chosen: benzophenone (E_T = 69.2 kcal mol^{-1}), 2-benzoylnaphthalene (E_T = 59.5 (non-polar solvent), 61.5 (polar solvent) kcal mol^{-1}), chrysene (E_T = 56.8 kcal mol^{-1}), dibenz[a,j]anthracene (E_T = 52.4 kcal mol^{-1}), fluoanthene (E_T = 52.4 kcal mol^{-1}), dibenzo[a,c]anthracene (E_T = 50.3 kcal mol^{-1}) and 1,2-benzanthracene (E_T = 47.2 kcal mol^{-1}); these were obtained from the laboratory stock of quenchers in Bordeaux (data from Ref. [17]).

Benzene (dielectric constant at 25 °C, ϵ^{25} = 2.28), cyclohexane (ϵ^{25} = 2.03), methanol (ϵ^{25} = 32.6) and ethanol (ϵ^{25} = 24.3) were of Uvasol quality; methyltetrahydrofuran (MTHF, Merck or Aldrich, ϵ^{25} = 7.6) was weakly fluorescing with a maximum near 350 nm on receipt. Purification steps included shaking with 2 N NaOH in water, drying with $CaCl_2$, storing overnight over solid KOH and distillation, and subsequent distillation over Na wire with nitrogen flushing. By storing the purified solvent under nitrogen, the appearance of spurious fluorescence was suppressed. Sodium dodecylsulphate (SDS) was purchased from Merck and purified by recrystallization from methanol.

2.2. Instrumentation and procedures

The absorption spectra at room temperature were taken using a Zeiss DMR 10 or a Hewlett-Packard diode array spectrometer and those at variable temperature with a Beckman Acta VI spectrophotometer. A Cryophysics cryostat was used to select different temperatures down to 70 K.

Transient absorption measurements were performed using a laser flash photolysis set-up with crossed beam arrangement. The sample in a 10 mm × 10 mm cell was excited at 355 nm by single light pulses (200 ps; 5–30 mJ) provided by a frequency-tripled, mode-locked Nd-YAG laser (Quantel). The detection system (pulsed Xe arc, monochromator, photomultiplier and Tektronix 7912 transient digitizer) had a response time of 3 ns.

Emission and emission excitation spectra were obtained using spectrofluorometers (Aminco, Farrand (Mark II) and Perkin Elmer (LS 50)) with the necessary accessories (low temperature spectra by immersion in liquid N_2; those at variable temperatures with the cryostat). The emission spectra were corrected by comparison with a quinine sulphate standard [18]. The quantum yields and P/F ratios were calculated from the integrals over the corrected emission bands on a wavenumber scale. Fluorescence decay times were measured by an ORTEC single-photon-counting equipment with a free running flash lamp (full width at half-maximum (FWHM), 1.5 ns) for excitation, and deconvoluted according to a least-squares method with a Fortran program by O'Connor and Philips [19]. Discrimination between monoexponential and biexponential decay kinetics was performed according to the magnitude of χ^2. The decay times of **1** were confirmed within ± 1 ns using the Bordeaux transient absorption set-up (without spectroflash, the recorded intensity is that of the emission). Phosphorescence decay times were determined in Hohenheim by a laser flash set-up (dye laser FL 2000 pumped by MSC 101 excimer laser (Lambda Physik), Tektronix 1103 oscilloscope, Tektronix digitizing camera and IBM PC) which has a time resolution of about 30 ns, and they were also in agreement with the data collected using the Bordeaux equipment. All samples were deaerated by flushing with nitrogen or argon.

For well deaerated solutions, all three molecules under investigation are stable on irradiation with a 75 W high pressure Hg lamp and 366, 405 and 436 nm filters for 30 min.

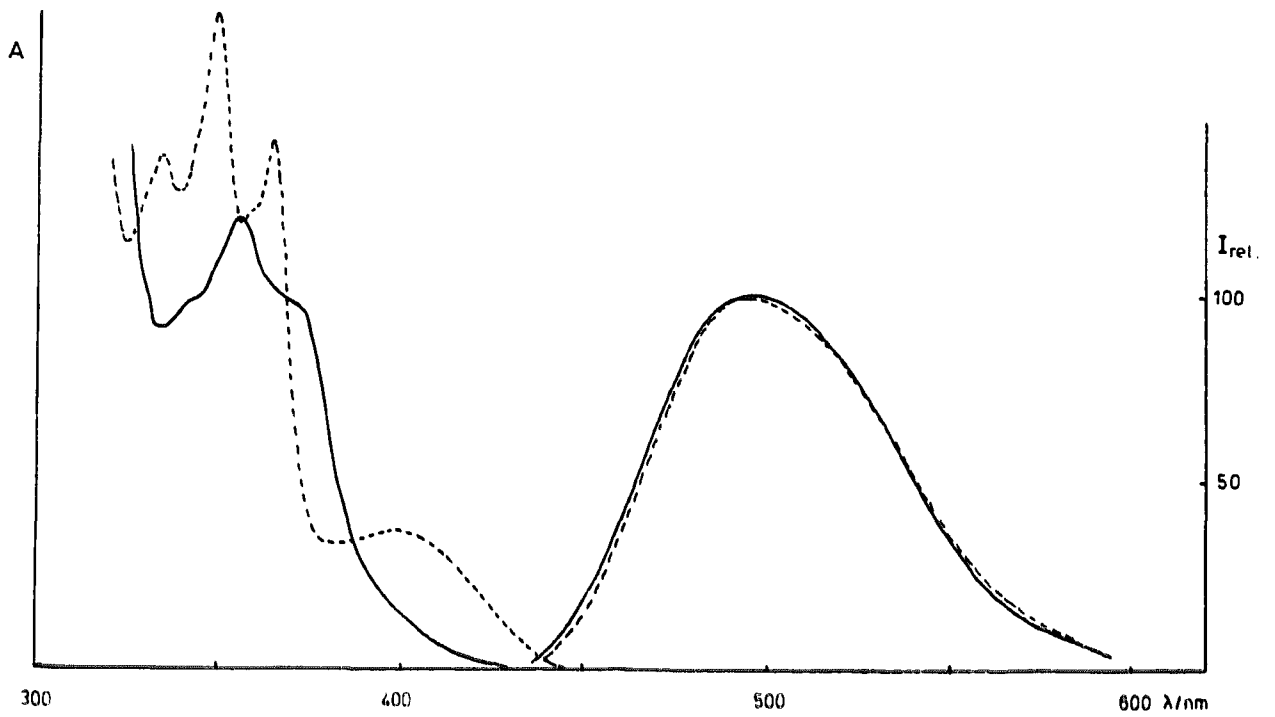

Fig. 1. Absorption and emission spectra of 1 in MTHF (– – –) and ethanol (——) at room temperature.

3. Results

3.1. Benzo[c]cinnoline (1)

The spectroscopy of this compound has been well studied [4,20–23]. Fig. 1 shows the absorption and uncorrected emission spectra in MTHF and ethanol. The n → π^* band is clearly separated from the $\pi \rightarrow \pi^*$ system; 1 thus belongs to the class of azobenzene-type azo molecules. It can be seen that the n,π^* transition in ethanol (about 400 nm) is strongly shifted towards higher energies compared with its position in MTHF (0–0 transition at 425 nm). At room temperature, the fluorescence wavelength of 1 is independent of the solvent (0–0 transition at about 425 nm, maximum at 495 nm). In a former paper, we have shown that the maximum of the fluorescence band is shifted to higher energies when the viscosity is increased by lowering the temperature [21]. These features have been rationalized by the concept that, in ethanol, the hydrogen-bonded species should absorb, but the hydrogen bond is broken during the lifetime of the excited (n,π^*) state and the non-bonded species should emit [4,21]. The quantum yield of fluorescence in ethanol (contrary to that in hydrocarbon solvents or completely esterified glycerin triacetate) shows a maximum as a function of decreasing temperature [21]. In order to determine whether a change in emitting state is responsible for this behaviour, we measured the lifetime of fluorescence in ethanol as a function of temperature (Fig. 2). We observed a maximum curve, which shows that the radiative lifetime τ_0 of the emitting species is constant: $\tau_0 = \tau/\phi = (4 \times 10^{-9}/0.0075)$ s = 500 ns. This is of the order of the radiative lifetime calculated from the absorption data [24] for the ^{1}(n,π^*) state in MTHF (ϵ_{max} = 350 l mol^{-1} cm^{-1}; $\Delta_{1/2}$ = 3300 cm^{-1}). This indicates emission from the (n,π^*) state at all temperatures. τ_0 is also independent of the excitation wavelength. In our experiments, we could not detect any phosphorescence emission.

In ethanol and benzene, a transient absorption is observed at room temperature which disappears with τ = 10 ns, virtually independent of the solvent. Its spectrum shows a maximum at 390 nm (Fig. 3). At wavelengths longer than 440 nm, the signal is obscured by fluorescence (τ = 4.5 ns in

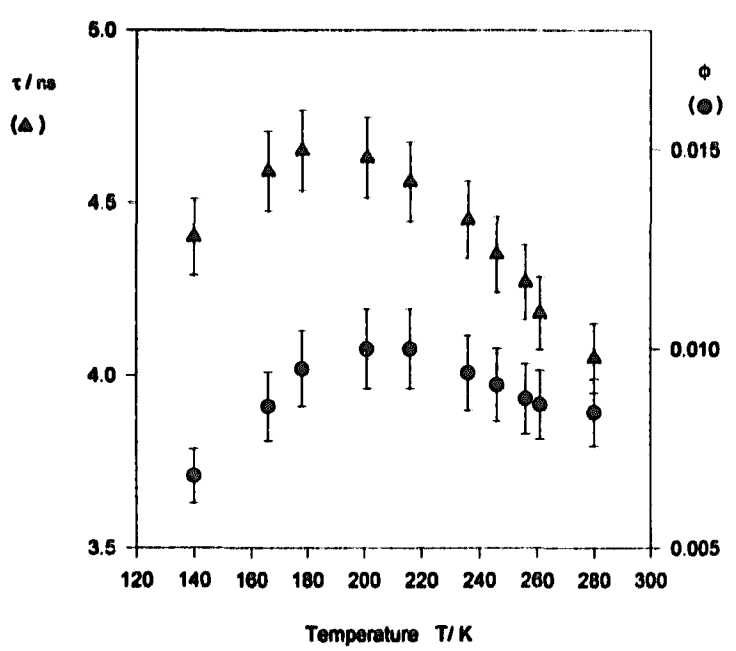

Fig. 2. Temperature dependence of the fluorescence lifetimes (▲) and quantum yields (●) [21] of 1. The error bars refer to 10% error in ϕ and 2.5% in τ.

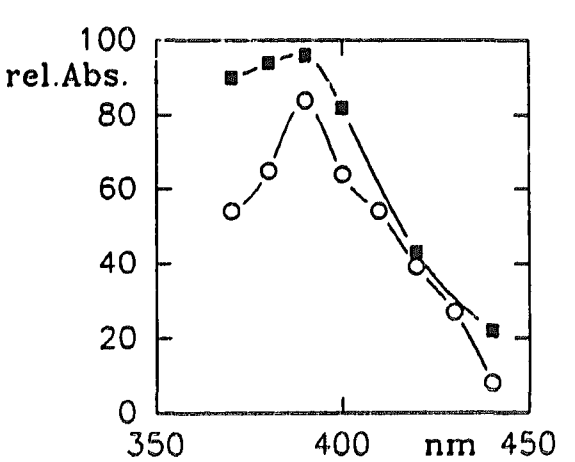

Fig. 3. Transient absorption spectra of 1 in cyclohexane (■) and methanol (○).

ethanol and 7 ns in benzene as determined with the experimental equipment used for transient absorption measurements; this should be compared with the value of 3.9 ns obtained by single photon counting; the value of 4.5 ns was obtained after correction of the measured value τ_{meas} by the relation $(\tau_{meas})^2 = \tau^2 + (\tau_{app})^2$ by the response time of the system $\tau_{app} = 3$ ns. The same correction with $\tau_{app} = 3.7$ ns would give $\tau = 3.94$ ns). In micellar solutions with an average occupation of five molecules of **1** per micelle, no transient is observed, probably due to concentration quenching; however, at a low occupation number of 0.38, where singly occupied micelles predominate, the lifetime of the transient is prolonged to $\tau \approx 17$ ns. On the basis of the difference between the lifetimes of fluorescence and the transient species, we assign the transient absorption to a $T_1 \rightarrow T_n$ absorption.

At low temperatures, triplet lifetimes normally increase because of the disappearance of collisional quenching. However, we were unable to detect a transient signal at temperatures as low as 120 K with the set-up in Hohenheim (carried out by Dr. R. Frank), whose time time limitation is 30 ns; thus the lifetime of the T_1 state seems to be determined by internal factors rather than by a diffusion-controlled process.

The energy of the lowest triplet state has been determined from experiments with **1** as a quencher of hydrocarbon triplets. In benzene, we found $E_T = 52$ kcal mol^{-1} (18 200 cm^{-1}) and in methanol $E_T = 51$ kcal mol^{-1} (17 900 cm^{-1}) with an estimated uncertainty of ± 1.5 kcal mol^{-1}. This is in agreement with the energy of the triplet state of **1** in polyalcohols [25]. Thus the energy of the triplet state is virtually unaffected by the solvent, which agrees well with the data in the literature [25] for $^3(n,\pi^*)$ as well as for $^3(\pi,\pi^*)$ states.

We should note that **1** is not really stable under all irradiation conditions; this is also true for **2**. This will be examined more closely in a later study.

3.2. Diaza[5]helicene (2)

In Fig. 4(a), we show the room temperature absorption spectra and uncorrected emission spectra of **2** at 77 K. For

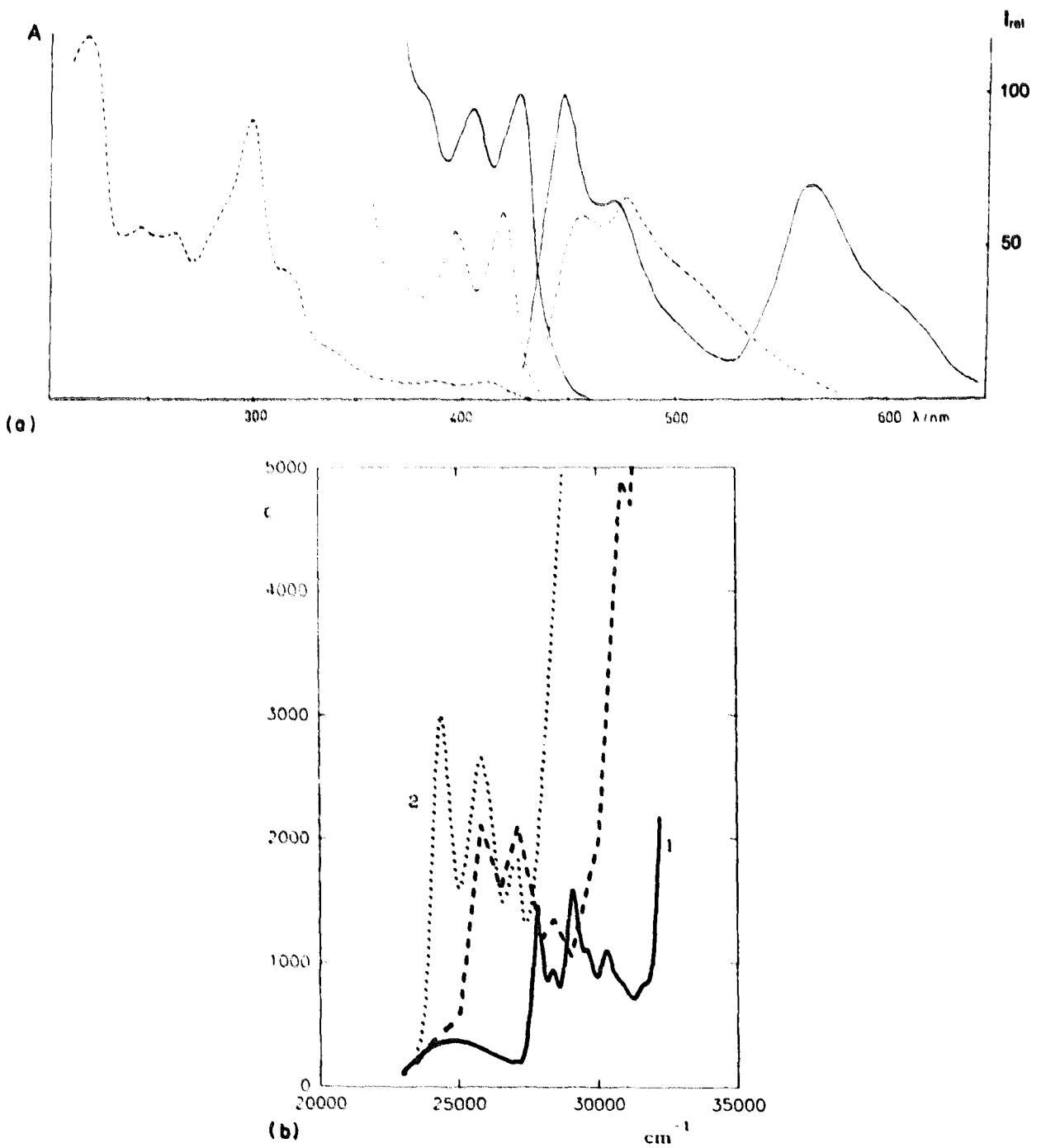

Fig. 4. (a) Room temperature absorption and 77 K emission spectra of 2 in MTHF (– – –) ($\epsilon_{417} = 2330$ l mol^{-1} cm^{-1}) and ethanol (——) ($\epsilon_{425} = 2340$ l mol^{-1} cm^{-1}). (b) Absorption spectra of 1 (——), naphtho[2,1-c]cinnoline (– – –) and 2 (· · · · ·) in *n*-hexane.

comparison, in Fig. 4(b), the absorption spectra of **1**, naphtho[2,1-c]cinnoline [26] and **2** in hexane are plotted. From this figure, it is clear that **2** belongs to the aminoazobenzene-type. Fig. 4(b) shows that, for **2** in non-polar solvents, the $^1(n,\pi^*)$ state is the lowest excited singlet state. The first vibronic band of the $\pi \rightarrow \pi^*$ transition peaks at 24 000 cm^{-1} (417 nm). In ethanol, we would expect a change in character of the lowest excited singlet state; the $\pi \rightarrow \pi^*$ band obscures the $n \rightarrow \pi^*$ transition as indicated by the solvent red shift of the $\pi \rightarrow \pi^*$ band by 500 cm^{-1} to 23 500 cm^{-1} (425 nm).

The fluorescence maxima at room temperature are at 21 900 cm^{-1} (457 nm) in MTHF and 22 500 cm^{-1} (445 nm) in ethanol. Thus the Stokes shift in MTHF is 2100 cm^{-1}, but only 1000 cm^{-1} in ethanol. The fluorescence decay times at room temperature are 1.1 ns in MTHF and 0.66 ns in ethanol; the quantum yields are 0.012 and 0.007 respectively. Thus the radiative lifetime τ_0 is about 100 ns and independent of the solvent. This is in agreement with the value calculated from the integrated $\pi \rightarrow \pi^*$ absorption band [24]. **2** shows phosphorescence at low temperature only in ethanol, not in MTHF. The P/F ratio (2.25 ± 0.25) is independent of the excitation wavelength.

2 shows transient absorption in benzene and methanol with $\tau = 20$ ns, which can be reduced to $\tau = 14$ ns by oxygen saturation (achieved by oxygen bubbling for 30 min). With these two points, and assuming an oxygen concentration of 10.1×10^{-3} mol dm^{-3} [17], an order of magnitude quenching constant of $k_q = 2 \times 10^9$ dm^3 mol^{-1} s^{-1} for oxygen is estimated according to the Stern–Volmer formula. This would indicate nearly diffusion-controlled oxygen quenching. On the basis of the different decay times of fluorescence and transient absorption, the transient absorption is assigned to a triplet species.

A rough comparison of the triplet formation yields in benzene and methanol is possible by comparing the maximum of the transient absorption signals provided that the experimental conditions are equal, which can be safely assumed in two successive experiments with equal absorbance of the solution at the excitation wavelength. It is found that the triplet formation yield does not differ widely, but is the same in both experiments within a factor of two. The triplet energy, as determined by quenching experiments, is 52.5 kcal mol^{-1} (18 400 cm^{-1}) in benzene and 53 kcal mol^{-1} (18 600 cm^{-1}) in methanol. The latter value is in agreement with that obtained from low temperature phosphorescence in ethanol.

3.3. Dibenzodiaza[7]helicene (3)

Fig. 5 gives the room temperature absorption spectra and uncorrected low temperature emission spectra of **3** in MTHF and ethanol. The absorption spectrum can be explained by the angular anellation of the aromatic systems; no indication of a low-lying $^1(n,\pi^*)$ state is visible. This puts **3** into the class of pseudo-stilbenes in the azo compound classification.

The maximum of the structureless fluorescence band at room temperature (Fig. 6) is at 485 nm in MTHF and 510 nm in ethanol. The absorption and emission spectra are both red shifted in the more polar solvent. Features quite unusual for aromatic ring systems are the gentleness of the long-wavelength slope of the absorption spectrum and the large Stokes shift at room temperature (Figs. 5(a) and 6). At low temperature, however, a new long-wavelength absorption band appears (Fig. 6) and, corresponding to this, a new short-wavelength fluorescence band develops in the fluorescence spectrum (Figs. 5 and 6), thus reducing the Stokes shift considerably. In ethanol, the fluorescence decay at room temperature is characterized by $\tau = 1.3$ ns and at 77 K by $\tau = 2.5$

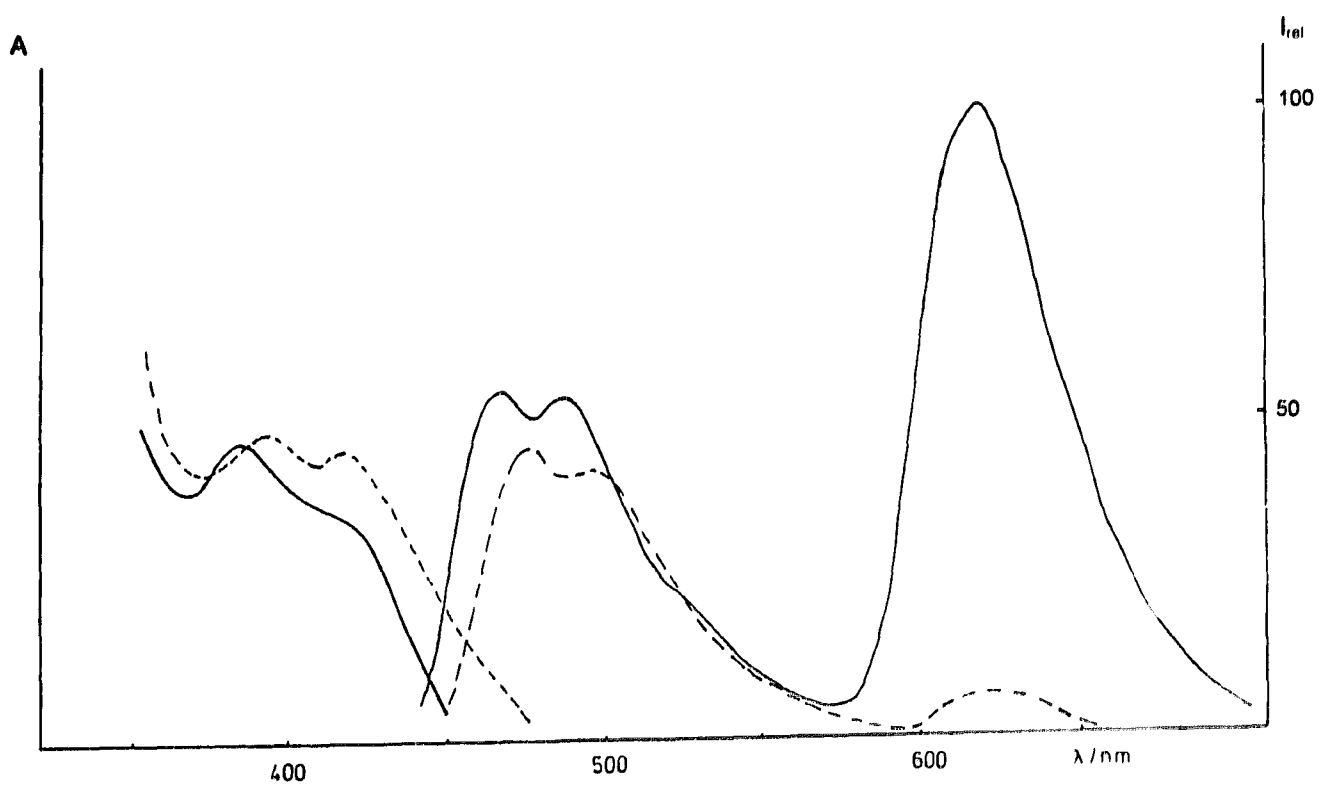

Fig. 5. Room temperature absorption and 77 K emission spectra of **3** in MTHF (——) ($\epsilon_{385} = 8380$ l mol^{-1} cm^{-1}) and ethanol (– – –) ($\epsilon_{395} = 5520$ l mol^{-1} cm^{-1}).

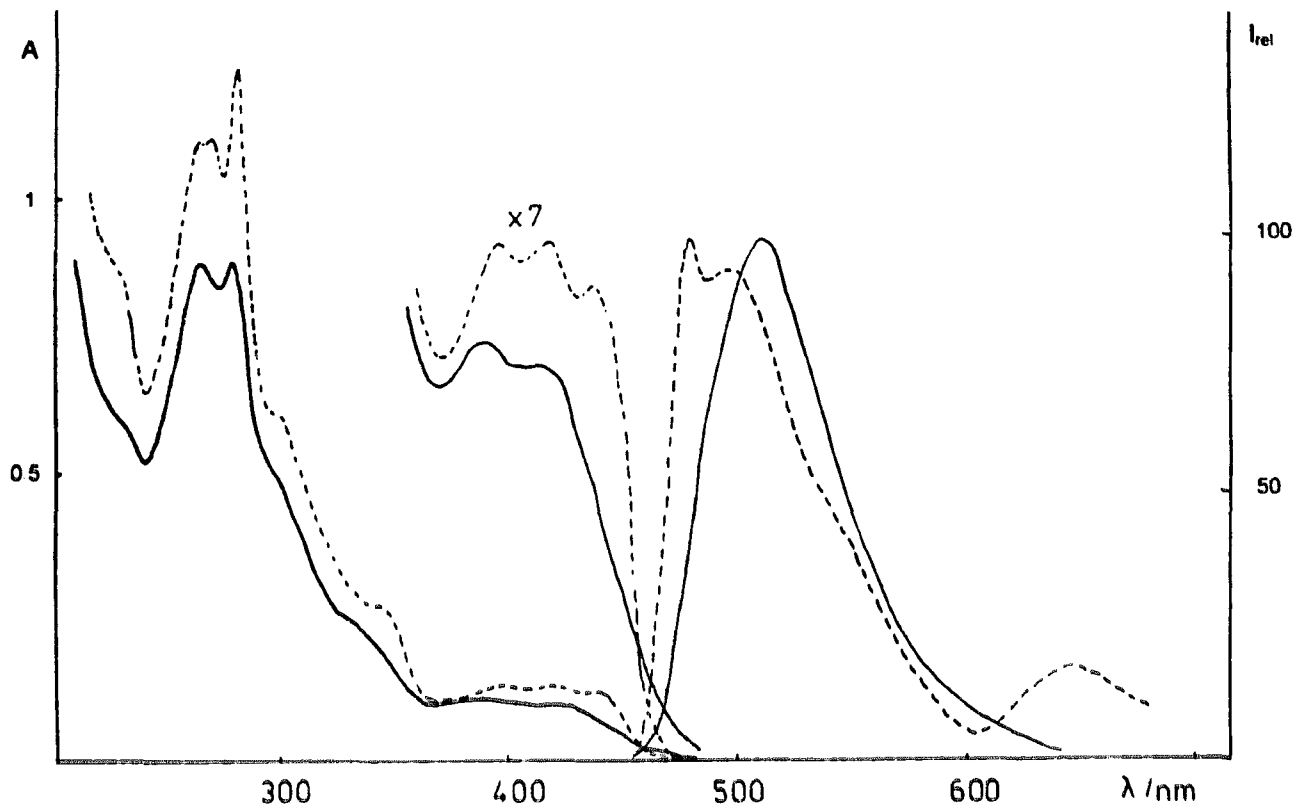

Fig. 6. Absorption and emission spectra of 3 in ethanol at room temperature (——) and 77 K (- - -).

Table 1
Spectral properties of 1, 2 and 3 at room temperature

Solvent	Compound	Fluorescence				Transients		P/F
		$\bar{\nu}$ (cm^{-1})	τ (ns)	ϕ	τ_0 (ns)	τ_{tr} (ns)	E_T (cm^{-1})	
Ethanol	1	23500	3.8	0.075	500	10	17800	0
	2	22500	0.66	0.007	95	20	18700	2.25
	3	19600	1.3	0.016	80	1000	16600	0.6
MTHF	1	23500	5.4			10	18300	0
	2	22000	1.1	0.012	100	20	18700	0
	3	20600	1.3/5.5	0.0016	800	5000	17200	13.5

ns. In MTHF at 298 K, we observe a biexponential decay with components of 1.3 ns (major component, 80%) and 5.3 ns (minor component, 20%); at 65 K, the data are $\tau_1 = 2.5$ ns (80%) and $\tau_2 = 5.0$ ns (each ± 0.5 ns) independent of the monitoring wavelength. The yield in ethanol is 0.016, but only 0.0016 in MTHF; thus τ_0 in ethanol is about 80 ns and about 800 ns in MTHF. Calculation of τ_0 from the lowest energy $\pi \rightarrow \pi^*$ absorption between 480 and 370 nm gives values of the order of 20 ns in both ethanol and MTHF. When the temperature is lowered slowly from 298 K to 77 K, there is a steady increase in the fluorescence yield of 3 in ethanol by about a factor of less than two, which matches the increase in the lifetime. Thus the decay of the fluorescing state is virtually non-activated. In this experiment, phosphorescence appears only at temperatures below 90 K, when ethanol is a rigid glass.

At room temperature, 3 shows a transient absorption in both benzene and ethanol solutions with $\tau \approx 5$ μs and $\tau \approx 10$ μs respectively. Comparison of the $T_1 \rightarrow T_n$ absorption signals shows that the triplet yield is comparable in both solvents. From the low temperature emission spectra, the triplet energy in MTHF is 49 kcal mol^{-1} (17 200 cm^{-1}) and in ethanol 47.5 kcal mol^{-1} (16 600 cm^{-1}). The phosphorescence lifetime at 77 K is 100 ms. A summary of most of the spectroscopic data is given in Table 1.

3 is chiral and can be resolved into its enantiomers [16]. Figs. 7(a) and 7(b) show the CD spectra of 3 at room temperature in ethanol and acidified ethanol [27] respectively.

3.4. The P/F ratio

The low temperature P/F ratios are highly solvent dependent (Table 2). 1 does not develop phosphorescence in non-polar solvents and normal alcohols, although phosphorescence has been reported in mixtures of normal and fluorinated alcohols due to stronger hydrogen-donating properties [28]; protonating solvents such as H_2SO_4, however, do not induce phosphorescence [29]. 2 shows phosphorescence only in polar solvents and 3 phosphoresces in both types of solvent.

The P/F ratio of 3 is dependent on the excitation wavelength (Fig. 8). This ratio is small at long excitation wave-

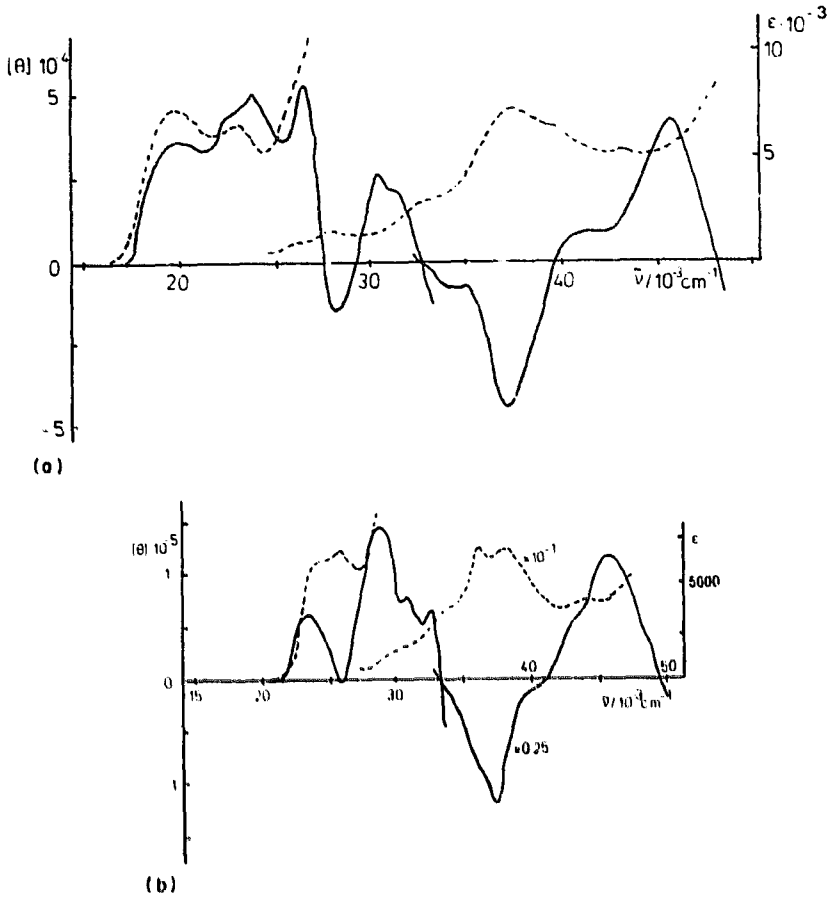

Fig. 7. (a) CD spectrum (—) and absorption spectrum (- - -) of 3 in ethanol. (b) CD spectrum (—) and absorption spectrum (- - -) of 3-H$^+$ in acidified ethanol.

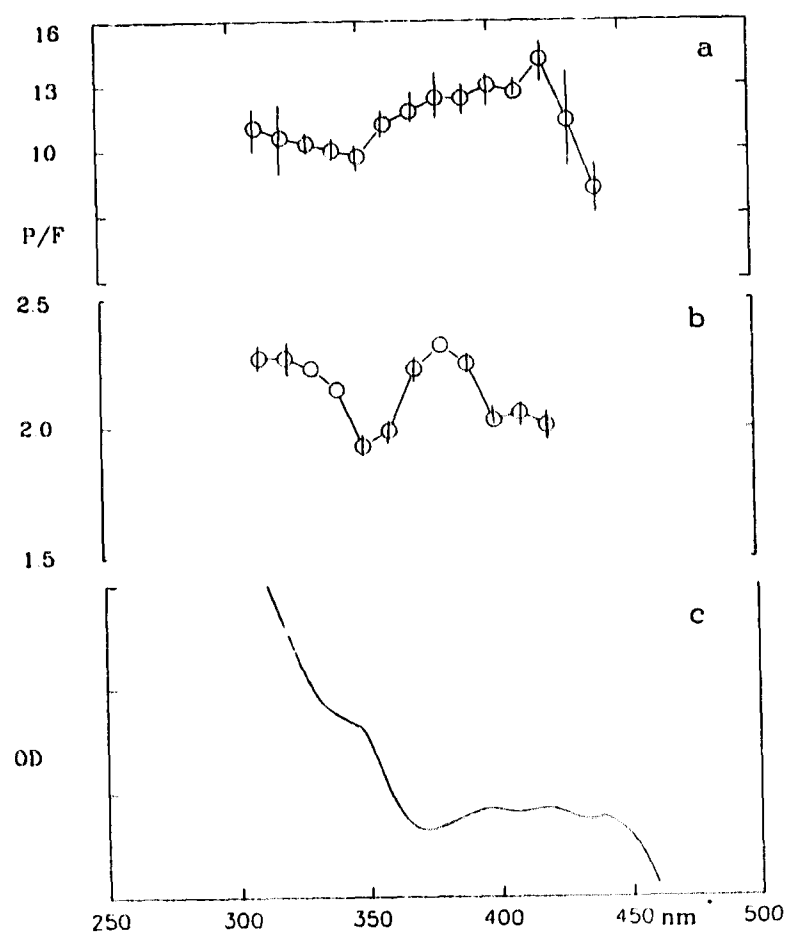

Fig. 8. P/F ratio of 3 at 77 K. Mean values of three determinations in MTHF (a) and ethanol (b) and room temperature absorption spectrum of 3 in ethanol (c). The error bars in (a) and (b) represent the maximum error.

lengths, but increases down to 420 nm. However, the data are uncertain at $\lambda > 420$ nm, because narrow slits had to be used and we were still unable to eliminate all scattering. A significant difference is seen in the plots for MTHF (Fig. 8(a)) and ethanol (Fig. 8(b)). However, in both plots the P/F ratio

Table 2
Corrected P/F ratios

Solvent	1	2	3 (380 nm excitation)
Ethanol	0	2.2	0.6
MTHF	0	0	13.5

is high in the region of 400 to 370 nm; a decrease follows between 370 and 340 nm and, at shorter wavelengths, the P/F ratio increases again. Such a phenomenon has not been observed previously to our knowledge. The P/F ratio vs. λ_{exc} plot in Fig. 8 was reproduced with different equipment (H. Rau at the Department of Chemistry, Washington State University, Pullman, Washington, with a Hitachi spectrofluorometer; G. Greiner and B. Knievel at the Institute of Chemistry, Hohenheim University, with a Farrand MK II spectrofluorometer; H. Rau and U. Radon at the same laboratory with an Aminco-Bowman spectrophotometer) with material which had been subjected to different purification procedures. We can safely exclude impurities and also photoproducts as we irradiated a sample in ethanol for 2.5 h with the 366 nm line of an St 41 Hg lamp and could not detect changes in the absorption or emission spectra.

3.5. Calculations of the state energies of 1–3

The recent advent of semiempirical programs for the calculation of molecular [illegible] and excited states provides a tool to check the empiri[illegible] state assignment (see below). Geometry optimization was carried out using the MM+ method in HyperChem. Spectroscopic calculations for the evaluation of the singlet and triplet state energies of **1**, **2** and **3** were made with the ZINDO/S program from the HyperChem package with the 1s orbitals of the H atoms and the 2s and 2p orbitals of the C and N atoms (64 orbitals for **1**, 100 for **2** and 172 for **3**). Interaction of 451 configurations was included in the calculations for **1–3**. The n or π nature of the calculated molecular orbitals was taken from the orbital contour maps, the main criterion being in-plane symmetry or antisymmetry at the nitrogen centres. The calculated states which may be of spectroscopic interest in this context are shown in Fig. 9.

The calculations predict the lowest singlet excited states of **1** and **2** to be of (n,π^*) type and that of **3** of (π,π^*) type; the lowest triplet states are of (n,π^*) type for **1** and of (π,π^*) type for **2** and **3**. These calculations are valid for the gaseous state, but the sequence of states on the energy scale should be the same in non-polar MTHF, whereas in ethanol the influence of the polar solvent may lead to a re-ordering of the states. It is interesting that the $n_n \rightarrow \pi^*$ transition in **3** is calculated to be the second or third transition, which is in agreement with the band assignment in the CD spectrum; the $n_s \rightarrow \pi^*$ band is at 230 nm (43 410 cm^{-1}).

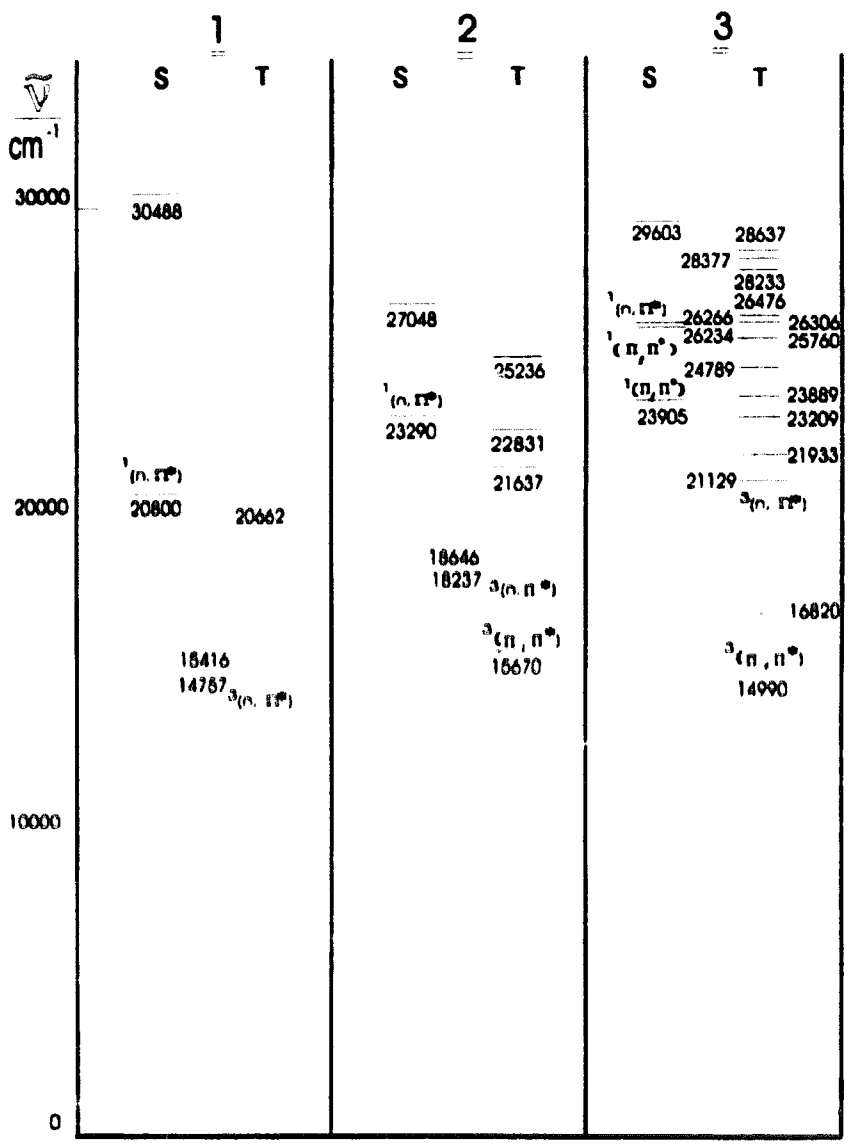

Fig. 9. Calculations with ZINDO/S for 1, 2 and 3. 15 occupied and 15 unoccupied orbitals included in CI. Torsion angle 20.6° for 2 and 19.9° for 3 as optimized by MM+.

4. Discussion

4.1. Absorption spectra and state assignment

The spectra of 1, 2 and 3 are related to those of the corresponding hydrocarbons phenanthrene [30], pentahelicene [15] and heptahelicene [31].

For 1 the n → π* band (maximum 420 nm) is well separated from the π → π* region in MTHF; it largely disappears in the π → π* absorption in the hydrogen-bonding solvent ethanol (λ_{max} about 390 nm) (Fig. 1). 1 belongs to the azobenzene-type azo compounds. In the absorption spectrum of 2, the n → π* band is at the long-wavelength end of the absorption region [32] in non-polar solvents, which is in agreement with the calculations (Fig. 4). Another hint that, in MTHF, the (n,π*) state is the lowest excited state may be seen in the large Stokes shift of the low temperature emission which is reduced in ethanol [5c]. Thus in MTHF the lowest excited singlet state is of (n,π*) character, whereas in ethanol it is of (π,π*) type, and 2 belongs to the aminoazobenzene-type azo compounds.

For 3 we observe a shift towards lower energy in both the absorption and the emission spectrum when ethanol replaces MTHF (Fig. 5), which indicates the (π,π*) character of the lowest excited state in both solvents. Corbett et al. [12a] stated that there should be a correlation between the appearance of an n → π* band and the deviation from molecular planarity of molecules with helicene character. We tried to obtain some information on the position of the n → π* band for 3 from the CD spectra of 3 in ethanol and 3-H$^+$ in acidified ethanol (Fig. 7). In these spectra, we observed a negative band centred around 25 300 cm^{-1} (395 nm) in the unprotonated molecule and around 27 800 cm^{-1} (360 nm) in the protonated molecule. This is expected for an n → π* transition. 3 belongs to the pseudo-stilbene class of azo compounds.

An assignment of the lowest triplet states to ^{3}(n,π*) or ^{3}(π,π*) does not seem possible on the basis of solvent effects. According to Ref. [17], the energy difference for both types of state on variation of the solvent is similar. However, a conflicting report by Stikeleather [33] states the same influence of solvent polarity on triplet states as is known for the singlets: for cinnoline and phthalazine in hydrocarbon solution, the ^{3}(n,π*) and ^{3}(π,π*) states are nearly degenerate, whereas in hydroxylic solvents the ^{3}(π,π*) state is the lowest. When we compare the diazaaromatic with the homoaromatic hydrocarbons (Table 3) we obtain, for the naphthalene series, ΔE_{S-T}(n,π*) values of 30–36 kcal mol^{-1} and ΔE_{S-T}(π,π*) values of 10–12 kcal mol^{-1}. Using

Table 3
Comparison of diazaaromatic and homoaromatic hydrocarbons

Compound	Absorption n → π* (kcal mol^{-1})	Absorption π → π* (kcal mol^{-1})	Triplet energy (kcal mol^{-1})
Naphthalene [a]	–	92	61
Cinnoline [b]	64.5	90	54
Phthalazine [c]	73.5	93	60.6
Phenanthrene [a]	–	82.5	62
1	63.5	79.5	51–52
Pentahelicene [d]	–	72	56.5
2	–	67.5	52–53

[a] Ref. [34].
[b] Ref. [35].
[c] Ref. [29].
[d] Ref. [15].

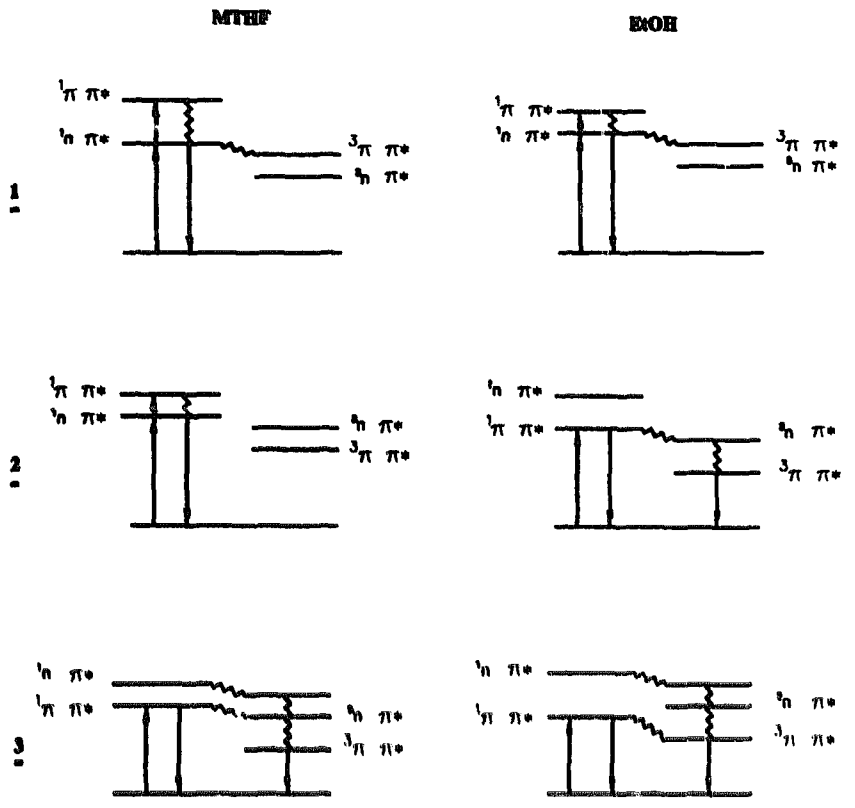

Fig. 10. State diagrams for 1, 2 and 3 derived from calculation and experiments in MTHF and ethanol: ~~~, radiationless transition; —, radiative transition. The strongest emission is indicated by a bold arrow.

the same numbers for the phenanthrene/1 pair, we would expect the lowest triplet state to be of $^3(n,\pi^*)$ character; in the pentahelicene/2 pair, both triplet states will be at similar energies. According to this reasoning, we have constructed the qualitative energy level diagrams of Fig. 10, which are in agreement with the calculations. This scheme will be the basis for the discussion of the photophysics of the azahelicenes. For 1 in ethanol, the triplet states are nearly degenerate; stronger hydrogen donors are required to shift the $^3(n,\pi^*)$ state to higher energies [33].

4.2. Emission properties

A common feature of all three molecules is their low emission yield (around 1%–2%). Such low yields are the exception rather than the rule for rigid aromatic molecules. Indeed, the parent hydrocarbons have considerably higher yields (phenanthrene, 20%; pentahelicene, 10%). It is known that nitrogen substitution and non-planarity promote intersystem crossing (ISC) and so high triplet populations are expected for the diazahelicenes. The close agreement between the fluorescence yields of 1–3 may be fortuitous as the emission originates in different types of state.

4.2.1. Benzo[c]cinnoline (1)

1 is the only planar C_{2v} molecule in the series. Here the El-Sayed rules [36] apply and indicate that ISC from the lowest $^1(n,\pi^*)$ to the $^3(\pi,\pi^*)$ state is favourable; according to the energetic order of these states, we expect a high ISC efficiency (Fig. 10). The population of the triplet state is demonstrated by the transient signal obtained in flash experiments, which is definitely longer lived (10 ns) than the fluorescence decay time (4 ns), but still very short compared with the lifetimes of transients of other planar aromatic molecules. Such a short-lived triplet transient indicates that internal factors dominate the deactivation of the triplet state, a conclusion which has been inferred by Lin and Stikeleather [28] to be due to a pseudo-Jahn–Teller effect [37]. At low temperatures, phosphorescence is not observed in either solvent and the lifetime of the transient species is not increased to at least 30 ns, the time limitation of our low temperature set-up. This also indicates fast intramolecular deactivation; diffusive quenching is unimportant.

A small part of the singlet population decays radiatively. The fluorescence of 1 is that of the free molecule (Fig. 1); in ethanol, an existing hydrogen bond is broken in the excited state before emission occurs [4,23]. In ethanol, 1 shows an unusual temperature dependence of the fluorescence yields [21] and lifetimes. The maximum curve of τ vs. T (Fig. 2) parallels that of ϕ_F vs. T. The temperature maxima of these plots correlate with the viscosity increase of the solvent ethanol and the blue shift of the emission band [21]. We have inferred that the impediment of breaking the hydrogen bond should cause a decrease in the fluorescence yield as only the free molecule emits. The new decay time data show that the radiative lifetime is constant; this means that the opening of a new deactivation channel for the emitting state at low temperature, not the production of the emitting species, is responsible for the observed emission feature. The shift of emission observed with decreasing temperature [21] indicates that the breaking of the hydrogen bond and solvent relaxation are not one process: production of the non-hydrogen-bonded emitting species is rapid; it is produced in a Franck–Condon solvent cage with subsequent relaxation of the solvent. At low temperature, the relaxation is slow and the unrelaxed OH-containing solvent assists in the deactivation of the emitting state.

4.2.2. Pentahelicene (2) and heptahelicene (3)

We may anticipate rather high ISC rates in 2 and 3 as the π systems are distorted (according to both calculated optimized geometries by about 20°) and favour the mixing of singlet and triplet states due to non-planarity [38]. Indeed, the triplet formation yield ϕ_T may be up to 0.90 for helicenes [39] and heteroatoms usually promote ISC even more. However, high triplet yields have been found only for the [5]- and [7]-, not the [4]-, [6]- or [8]-helicenes, which may indicate certain special features of those helicenes with an odd number of rings. Grellmann et al. [15] give an estimate of the phosphorescence yield $\phi_P = 0.15$ for [5]-helicene. Thus there is an effective deactivation channel for the lowest triplet state in [5]- and [7]-helicenes. For 2 and 3, we observe only weak phosphorescence at 77 K which, moreover, seems to be coupled to the strength of fluorescence.

The fluorescence lifetime of 2 at room temperature is about a factor of 20 smaller than that of [5]-helicene, and the radiative lifetime of 2 is in agreement with that calculated

from the $\pi \rightarrow \pi^*$ absorption band in MTHF as well as in ethanol. However, in MTHF, where the lowest excited singlet state is of $^1(n,\pi^*)$ character, a much longer lifetime would be expected. Nevertheless, we must not forget that the $^1(n,\pi^*)$ and $^1(\pi,\pi^*)$ states are practically degenerate. The pseudo-Jahn–Teller effect on the two singlet states, also discussed by Stikeleather [33], would lead to coupling of the two states and the shorter lived state would determine the decay kinetics. According to Ref. [33], the pseudo-Jahn–Teller effect would lead to better coupling to the ground state and increase the direct internal conversion (IC). At the same time non-planarity relaxes the El Sayed rules, so that Jahn–Teller-induced IC and ISC compete. The lifetime of the triplet is still very short (20 ns), which again indicates fast intramolecular deactivation of the triplet state. In ethanol, the $^3(n,\pi^*)$ state is expected to be shifted somewhat to higher energy; phosphorescence is observed.

For **3** we calculate $\tau_0 = 20$ ns from the integrated absorption of what seems to be the lowest $\pi \rightarrow \pi^*$ band (480 to 370 nm); however, τ_0 calculated from τ and ϕ is much longer. This seems to indicate that the absorbing and emitting singlet states in **3** are not identical, and that a state carrying lower oscillator strength contributes to the emission. Indeed, a low intensity band may be hidden in the unusually gentle slope of the long-wavelength end of the spectrum. The spectrum of **3** increases in intensity in this region on cooling; in ethanol, a new band or partial band appears (Fig. 6). It seems that more than one state is involved; the biexponential decay of **3** supports this suggestion.

In the ineffective (1%–2%) radiative channels, the a location of emission to singlets and triplets seems to be governed by ISC. The features of the radiative channels can be understood by using the conventional concepts of state stabilization by solvents and the El-Sayed rules for ISC [36] which predict preferred ISC between (n,π^*) and (π,π^*) states compared with ISC between like states. From our experiments and calculations, we have presented in Fig. 10 an ordering of the lowest excited states which rationalizes the observations.

4.3. The P/F ratio

For **2**, the P/F ratio is independent of the excitation wavelength as is expected for molecules obeying Kasha's rule. For **3**, this ratio is wavelength dependent (Fig. 8). We have excluded the fact that an impurity may have caused this behaviour, and have not observed any indication of association in these solid solutions.

Reports of an increase in the P/F ratio on excitation of higher states [40] can be rationalized by the assumption of a finite singlet–triplet transition probability in higher excited states. However, a decrease as shown in Fig. 8 near 350 nm has, to our knowledge, never been observed previously. Such a decrease means that either the excitation of higher states stimulates the fluorescence of the lowest excited state or opens up an additional channel of depopulation of the lowest triplet state. However, such an influence of the population of higher excited singlet states on the emission of the lowest excited singlet and/or triplet states is difficult to visualize.

Fig. 8(b) may provide a clue. In ethanol, there is a long-wavelength excitation region with a P/F ratio of about 2.0. If this is considered to be the P/F ratio on excitation of the lowest singlet state (determined by the ISC of the lowest excited singlet state and the deactivation efficiency of the lowest triplet state), then there is an increase in the P/F ratio below 400 nm. Singlet–triplet ISC in excited states at this energy may cause a relatively higher triplet yield. Near 350 nm, the P/F ratio is reduced to 2.0; states in this energy region deactivate completely to the lowest excited state by efficient IC. The P/F ratio increases again on excitation of states below 450 nm. In these non-planar aromatics, ISC seems to be possible not only in the lowest excited singlet state. The MTHF results in Fig. 8(a) do not show an excitation region of low P/F ratio at the long-wavelength end of the absorption spectrum, only a decrease in the P/F ratio. Tentatively, we infer the same concept, as towards 350 nm there is definitely a low P/F ratio.

5. Conclusions

The unusual spectroscopic properties of the *o*-diazahelicenes of this series can be rationalized by inferring the presence of at least two singlet states which are relatively close at low excitation energies. State mixing and efficient ISC lead to a low overall emission yield which must be discussed with regard to the non-planarity of the π systems. We expect, parallel to the homohelicene series, new information from investigations of diazahelicenes with even numbers of aromatic rings and of diazahelicenes which lack C_2 symmetry.

Acknowledgements

H.R. thanks Professor G. Crosby, Washington State University, Pullman, Washington, USA for his hospitality, Dr. Mikes for the work on chiral chromatography and Mrs. U. Radon, E. Hirsch and B. Wörner for help with the experiments.

References

[1] (a) J. Griffiths, *Chem. Soc. Rev.*, *1* (1972) 481; (b) H. Rau, Azo compounds, in H. Dürr and H. Bouas-Laurent (eds.), *Photochromic Materials: Theory and Application*, Elsevier, Amsterdam, 1989; (c) H. Rau, Photoisomerization of azobenzenes, in J.F. Rabek (ed.), *Photochemistry and Photophysics*, Vol. II, CRC Press, Boca Raton, 1989.

[2] E. Haselbach and E. Heilbronner, *Helv. Chim. Acta*, *53* (1970) 684–695.

[3] H. Rau and E. Lüddecke, *J. Am. Chem. Soc.*, *104* (1982) 1616–1620.

[4] E. Lippert and W. Voss, *Z. Phys. Chem. NF (Wiesbaden)*, *31* (1962) 321–327.

[5] (a) H. Rau, *Ber. Bunsenges. Phys. Chem.*, *71* (1967) 48–53; (b) H. Rau, *Ber. Bunsenges. Phys. Chem.*, *72* (1968) 637–643; (c) H. Bisle, M. Römer and H. Rau, *Ber. Bunsenges. Phys. Chem.*, *80* (1976) 301–305.
[6] H. Rau, *Angew. Chem.*, *85* (1973) 248–258.
[7] M.F. O'Dwyer, M.A. El-Bayoumi and S.J. Strickler, *J. Chem. Phys.*, *36* (1962) 1395.
[8] H. Rau and F. Totter, *J. Photochem. Photobiol. A: Chem.*, *63* (1992) 337–347.
[9] Houben-Weil, *Methoden der Organischen Chemie*, Bd 10, Teil 3, S. 354.
[10] G.E. Lewis, *Tetrahedron Lett.*, *9* (1960) 12; *J. Org. Chem.*, *25* (1960) 2193.
[11] *DMS-UV-Atlas*, Butterworths/Verlag Chemie, Spectrum No. H22/50.
[12] (a) F.F. Corbett, P.F. Holt and A.N. Hughes, *J. Chem. Soc.*, (1961) 1363; (b) P.F. Holt and M.R. Oatham, *J. Chem. Soc.*, (1963) 4099.
[13] F. Mikes and G. Boshart, *J. Chem. Soc., Chem. Commun.*, (1978) 173.
[14] J. Braithwaite and P.F. Holt, *J. Chem. Soc.*, (1959) 3025.
[15] K.H. Grellmann, P. Hentzschel, T. Wismontski-Kittel and E. Fischer, *J. Photochem.*, *11* (1979) 197–231.
[16] H. Rau and O. Schuster, *Angew. Chem.*, *88* (1976) 90; *Angew. Chem. Int. Ed. Engl.*, *15* (1976) 114.
[17] S.L. Murow, *Handbook of Photochemistry*, Marcel Dekker, New York, 1973.
[18] E. Lippert, W. Nägele, I. Seibold-Blankenstein, U. Staiger and W. Voss, *Z. Anal. Chem.*, *170* (1959) 1.
[19] D.V. O'Connor and D. Philipps, *Time Correlated Single Photon Counting*, Academic Press, 1984.
[20] E.M. Kreidler, *Thesis*, Stuttgart, 1965.
[21] H. Rau and H. Bisle, *Ber. Bunsenges. Phys. Chem.*, *77* (1973) 281–283.
[22] D.N. DeVries Reilingh, R.P.H. Rettschick and G.J. Hoytink, *J. Chem. Phys.*, *54* (1971) 2722.
[23] C. Mugiya and H. Baba, *Bull. Chem. Soc. Jpn.*, *40* (1967) 2201.
[24] S.J. Strickler and R.A. Berg, *J. Chem. Phys.*, *37* (1962) 814.
[25] H. Inoue, J.Y. Hiroshima and N.K. Tomiyama, *Bull. Chem. Soc. Jpn.*, *54* (1981) 2209–2210.
[26] *DMS-UV-Atlas*, Butterworths/Verlag Chemie, Spectrum No. H22/49.
[27] O. Schuster, *Thesis*, Tübingen, 1976.
[28] C.T. Lin and J.A. Stikeleather, *Chem. Phys. Lett.*, *38* (1976) 561.
[29] H. Rau, *Ber. Bunsenges. Phys. Chem.*, *72* (1968) 408–414.
[30] H. Zimmermann and N. Joop, *Ber. Bunsenges. Phys. Chem.*, *65* (1961) 66.
[31] R.H. Martin and M.J. Marchant, *Tetrahedron*, *30* (1974) 343.
[32] Badger and Walker, *J. Chem. Soc.*, (1956) 122.
[33] J.H. Stikeleather, *Chem. Phys. Lett.*, *24* (1974) 253–256.
[34] J.B. Birks, *Photophysics of Aromatic Molecules*, Wiley, New York, 1970, Table 3.1, p. 70.
[35] J.C.S. Wait and F.M. Grogan, *J. Mol. Spectrosc.*, *24* (1967) 383–401.
[36] (a) M.A. El-Sayed, *J. Chem. Phys.*, *36* (1962) 573; (b) M.A. El-Sayed, *J. Chem. Phys.*, *38* (1963) 2834; (c) M.A. El-Sayed, *J. Chem. Phys.*, *41* (1964) 2462.
[37] Y.H. Li and E.C. Lim, *Chem. Phys. Lett.*, *9* (1971) 279.
[38] O.E. Weigang, J.A. Turner and P.A. Trouard, *J. Chem. Phys.*, *45* (1966) 1126.
[39] (a) M. Sapir and E. Van der Donckt, *Chem. Phys. Lett.*, *36* (1975) 108; (b) E. Van der Donckt, J. Nasielski, J.R. Greenleaf and J.B. Dirks, *Chem. Phys. Lett.*, *18* (1968) 409.
[40] (a) H. Rau and L. Augenstein, *J. Chem. Phys.*, *46* (1967) 1773–1778; (b) J. Ferguson, *J. Mol. Spectrosc.*, *3* (1959) 177.